

# Deep water gravity wave triad resonances on uniform flow

David M. Kouskoulas<sup>1,\*</sup> and Yaron Toledo<sup>1,†</sup>

September 19, 2019

<sup>1</sup>Marine Engineering and Physics Laboratory, School of Mechanical Engineering, Tel Aviv University, Tel Aviv 6997801, Israel

## Abstract

Triad resonances for gravity waves propagating in opposite direction with respect to uniform current are introduced. They are produced by multivalued and anisotropic dispersion and occur even in deep water. In contrast, existing literature suggests non-degenerate deep water triads require inhomogeneity or capillary effects. In this sense, the new resonances are a first of their kind. Analytical conditions for the existence of resonance may be reduced to universal constants. Solution of a three-wave interaction model, adapted to the wave-current problem, shows regimes wherein the dominant direction, speed and strength of resonant energy transfer differs between wavenumber scales. This suggests uniform current is a fundamental source of spatial inhomogeneity. The new resonances significantly modify the picture of nonlinear interactions in wave-current fields. Since the resonances are quadratic, they will also dominate well known quartet interactions.

## 1 Introduction

Water waves often propagate on flows. The transformation of the single-valued water wave dispersion relation to a multi-valued and anisotropic form when accounting for mean motion is well known [cf. Kitaigorodskii et al., 1975, Peregrine, 1976]. Nonlinear interactions involving the “small” wavenumber solutions have been shown to produce new spatiotemporal features in wave fields [Kouskoulas and Toledo, 2017]. Similarly, for ships moving with constant velocity, multi-valued dispersion solutions are of known importance to heave and pitch ship motions [Newman and Sclavounos, 1980] and wave diffraction by slender bodies [Sclavounos, 1981b,a]. Wave-current experiments have demonstrated the effects of current direction on Bragg resonance [Rey et al., 2002, Magne et al., 2005]. Current inhomogeneities have also been shown to produce resonance by means of wave trapping [Shrira and Slunyaev, 2014] and vorticity waves [Drivas and Wunsch, 2015].

Resonances are understood to be a dominant mechanism of energy transfer [Hasselmann, 1962]. Accordingly, current effects on resonance are of significant importance. Resonance conditions occur when dispersion permits phase matching between linear and nonlinear terms. This phase matching results in growth of nonlinear terms [Phillips, 1960]. If the interaction time is sufficiently long, higher order terms

---

\*dkouskoulas@mail.tau.ac.il

†toledo@tauex.tau.ac.il

may grow to first-order magnitude [Benney, 1962]. Resonant energy exchange has been shown for gravity-capillary waves [McGoldrick, 1965], surface and internal waves [Alam et al., 2010], and antiparallel acoustic and gravity waves [Kadri and Stiassnie, 2013, Kadri and Akylas, 2016]. Resonances, in 2DH problem, have also been suggested near the cusp line of Kelvin ship waves [Newman, 1970]. In deep water, degenerate triad resonances have been discussed [Longuet-Higgins, 1962]. However, existing literature suggests there is no non-degenerate resonance for deep water gravity waves without inhomogeneity (i.e. current shear) or capillary effects. In contrast, it will be shown that nontrivial gravity wave triads exist for uniform flows in intermediate and even deep water.

The existence of nontrivial deep water gravity wave triad resonance on uniform current is demonstrated. They occur between gravity waves propagating in opposite directions with respect to current even in deep water. In §2, the linear wave-current dispersion relation is reviewed. It is shown to be multi-valued and anisotropic. In §3, a geometric approach demonstrates the existence of resonance. In §4, resonance conditions are found for a laboratory viewer. They exist among, but not between, two wave mode types. If the ratio between initial harmonics is known, conditions reduce to universal constants. In order to demonstrate consistency between inertial viewers, resonance conditions for an observer moving with the current velocity is derived in §5. Amplitude coupling and energy exchange is shown in §6. Resonant behavior differs between wavenumber scales. A conclusion and discussion is given in §7. The new resonances preclude more complex 3D-effects and their weak nonlinearity would dominate known quartet interactions. Accordingly, results suggest multivalued and anisotropic dispersion may profoundly modify the dominant energy transfer mechanisms in wave-current fields.

## Preliminary remarks on Galilean invariance

Since the functional form of the single-valued plane wave dispersion relation does not permit for a nontrivial deep water triad resonance, it is perhaps tempting to assume the following results imply a violation of Galilean invariance. However, resonance conditions are found by satisfying the basic interaction condition and the relevant dispersion relations for each wave. Galilean invariance does not guarantee invariance of the functional form of the latter.<sup>1</sup> This is known in the transformation of the single-valued dispersion relation to a multi-valued form<sup>2</sup> in the presence of mean motion [cf. Kitaigorskii et al., 1975, Peregrine, 1976, Newman and Sclavounos, 1980, Sclavounos, 1981b,a, Peregrine and Jonsson, 1983]. If the Galilean transformation guaranteed invariance of the dispersion relation's functional form, one of these would be invalid. In fact, the single-valued case is just a degenerate case in the mathematical limit of zero current.

On account of the (single-valued) intrinsic frequency dispersion function being only a degenerate case of the multi-valued form, caution must be taken when superposing intrinsic frequency representations. The intrinsic frequencies of opposing plane waves on current are described by different *locally* comoving observers [definition in Bretherton and Garrett, 1968]: one for waves following, and one for waves opposing current<sup>3</sup>. For a consistent description of the system, one must commit to a single observer. If one chooses the comoving observer for a wave following current, all waves following the current will not “feel” the mean motion; their dispersion relation will be the single-valued degenerate case. At the same time, since the system is not a rigid body, waves opposing the current will “feel” a mean motion relative to the observer. Hence, their dispersion will require the multi-valued form. The correct form of dispersion, for each direction

<sup>1</sup>The strict definition of invariance of dispersion for waves in moving media has been discussed by Censor [1980, 1998], McCall and Censor [2007].

<sup>2</sup>The single-valued dispersion relation form referred to is  $\sigma = \sqrt{gk \tanh kh}$ . The multi-valued form is  $\omega = \pm kU + \sqrt{gk \tanh kh}$ .

<sup>3</sup>The two comoving observers are found through application of a Galilean transformation in different directions with respect to current, which is defined by the laboratory observer.

of wave motion, is essential in determining resonance conditions. If the dispersion relations of all waves composing a resonance condition are derived from the same governing equations, Galilean invariance is not violated.

## 2 Linear formulation

The linear wave-current dispersion relation is derived using a velocity potential approach. It is shown to be multivalued and anisotropic.

### 2.1 Linear wave-current dispersion

Assume wave propagation with a uniform current in water of constant depth  $h$ . Irrotational and inviscid flow is assumed.  $x$  and  $z$  are horizontal and vertical coordinates respectively.  $\phi(x, z, t)$  is a velocity potential and  $\eta(x, t)$  is the surface elevation. The boundary value problem is given by [cf. Whitham, 1962]

$$\nabla^2 \phi = 0, \quad -h < z < \eta, \quad (1)$$

$$-\frac{\partial \phi}{\partial z} = 0, \quad z = -h, \quad (2)$$

$$\frac{\partial \phi}{\partial z} - \frac{\partial \eta}{\partial t} - \frac{\partial \phi}{\partial x} \frac{\partial \eta}{\partial x} = 0, \quad z = \eta, \quad (3)$$

$$\frac{\partial \phi}{\partial t} + \frac{1}{2} (\nabla \phi)^2 + g\eta + Q(t) = 0, \quad z = \eta. \quad (4)$$

Define flow quantities as power series in the small parameter  $\varepsilon = ka$ .

$$\phi = Ux + \varepsilon \tilde{\phi}, \quad (5)$$

$$\eta = \varepsilon \tilde{\eta}. \quad (6)$$

The current velocity  $U$  has been introduced in (5). Substituting (5) and (6) into Taylor series expansions of (3) and (4) yields

$$\frac{\partial \tilde{\phi}}{\partial z} - \frac{\partial \tilde{\eta}}{\partial t} - \left( U + \frac{\partial \tilde{\phi}}{\partial x} \right) \frac{\partial \tilde{\eta}}{\partial x} + \tilde{\eta} \frac{\partial^2 \tilde{\phi}}{\partial z^2} = 0, \quad z = 0, \quad (7)$$

$$\frac{\partial \tilde{\phi}}{\partial t} + U \frac{\partial \tilde{\phi}}{\partial x} + \frac{1}{2} \left( \frac{\partial \tilde{\phi}}{\partial x} \right)^2 + g\tilde{\eta} + \tilde{\eta} \frac{\partial^2 \tilde{\phi}}{\partial z \partial t} + U \tilde{\eta} \frac{\partial^2 \tilde{\phi}}{\partial x \partial z} = 0, \quad z = 0. \quad (8)$$

Eliminating  $\tilde{\eta}$  allows one to combine (7) and (8) into a single equation of the form

$$\mathcal{L}(\tilde{\phi}) + \mathcal{P}^2(\tilde{\phi}, \tilde{\phi}) = 0, \quad z = 0. \quad (9)$$

$\mathcal{L}(\cdot)$  and  $\mathcal{P}^2(\cdot)$  are linear and quadratic nonlinear operators respectively. Quadratic nonlinear terms are neglected in the linear approximation. The linear operator is

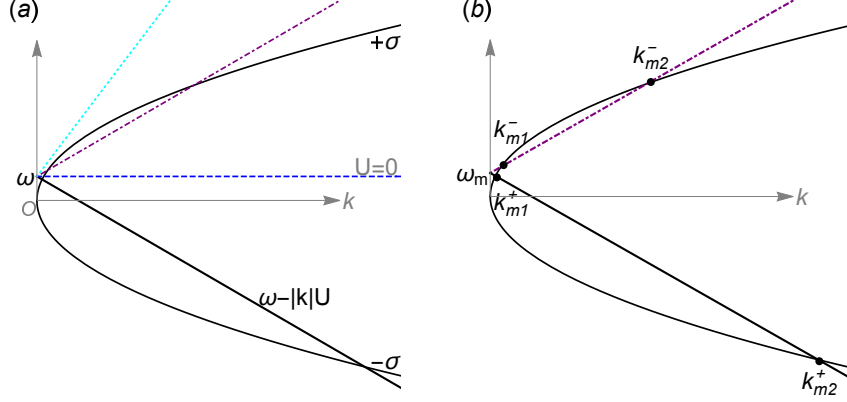


Figure 1: Graphical solution of wave-current dispersion relation. Intersections of  $y = \omega - kU$  with  $\sigma = \pm (gk)^{1/2}$  give wavenumber solutions.  $+U$  and  $-U$  correspond to wave motion following and opposing current respectively. (a) Solution branches for various  $U$ . A single branch may give two; black and purple dot-dashed lines, one; blue dashed line; or zero; cyan dotted line, solutions. (b) Wave motion following and opposing current (antiparallel wave motion) is given by two solution branches and may yield up to four nontrivial wavenumbers for a single frequency.

$$\mathcal{L}(\tilde{\phi}) = \frac{\partial^2 \tilde{\phi}}{\partial t^2} + g \frac{\partial \tilde{\phi}}{\partial z} + 2U \frac{\partial^2 \tilde{\phi}}{\partial x \partial t} + U^2 \frac{\partial^2 \tilde{\phi}}{\partial x^2}, \quad z = 0. \quad (10)$$

The nonlinear terms who compose  $\mathcal{P}^2(\cdot)$  are shown in Appendix D. A linear deep water solution for  $\mathcal{L}(\tilde{\phi}) = 0$  is well known,

$$\tilde{\phi} = a(c - U) e^{|k|z} \sin(kx - \omega t). \quad (11)$$

$a$  is the amplitude,  $c$  is the wave celerity,  $k$  is the wavenumber and  $\omega$  is the absolute frequency. Equations (11) and (10) yield the linear wave-current dispersion relation,

$$\omega - kU = \pm \sigma = \pm \sqrt{g|k|}. \quad (12)$$

$\sigma$  is the intrinsic frequency. Equation (12) is solved graphically by plotting  $y = \omega - kU$  and  $\sigma = \pm \sqrt{g|k|}$ . Wavenumber solutions are given by the points of intersection (see fig. 1a). “Small” and “large” wavenumber solutions, for each direction of  $U$ , are referred to as type I and type II modes respectively. These two pairs of wavenumbers are propagating in opposite directions with respect to current. Moreover, their magnitudes differ for following ( $U > 0$ ) and opposing ( $U < 0$ ) current. Thus, wave motion in two directions with respect to current may yield a total of four nontrivial wavenumber solutions (see fig. 2b).

## 2.2 Analytical solution for laboratory viewer

The laboratory viewer sees the fluid move with velocity  $U$ . The relevant dispersion relation, (12), may be written as

$\mathcal{D}(k, \omega, U)$				
	$n$	$U$	$k_{mn}^{\pm}$	mode type
$k_{m1}$	1	+	$\frac{g+2U\omega_m-\sqrt{g(g+4U\omega_m)}}{2U^2}$	I
$k_{m2}$	2	+	$\frac{g+2U\omega_m+\sqrt{g(g+4U\omega_m)}}{2U^2}$	II
$k_{m1}^-$	1	-	$\frac{g-2U\omega_m-\sqrt{g(g-4U\omega_m)}}{2U^2}$	I
$k_{m2}^-$	2	-	$\frac{g-2U\omega_m+\sqrt{g(g-4U\omega_m)}}{2U^2}$	II

Table 1: Wavenumber solutions for  $\mathcal{D}(k, \omega, U)$  using a positive wavenumber convention. Laboratory viewer,  $\mathcal{D}$ , sees four non-trivial positive wavenumber solutions.  $n = 1$  and  $n = 2$  are “small” and “large” wavenumber solutions (“short” and “long” wave solutions). Waves opposing current are defined by  $-U$ , waves following current are given by  $U$ .

$$D(k, \omega, U) = \omega = kU + \sqrt{g|k|}. \quad (13)$$

One may assume only positive wavenumbers. In this convention, waves propagating in opposite directions will both have positive wavenumbers, but will be functions of opposite signs of  $U$ .<sup>4</sup> In polynomial form (13) is

$$\mathcal{D}(k, \omega, U) = U^2 k^2 + (-2U\omega - g)k + \omega^2 = 0. \quad (14)$$

Since a positive wavenumber convention is used, the absolute value is dropped but still implied. As was shown graphically in §2, 14 is multi-valued. Moreover, the magnitude of these multiple solutions differs for a change in sign of  $U$ . The four nontrivial solutions for (14) may be written most succinctly in analytical form as

$$k_{mn}^{\pm} = \frac{g \pm 2U\omega_m + (-1)^n \sqrt{g(g \pm 4U\omega_m)}}{2U^2}, \quad n = 1, 2. \quad (15)$$

Wherein, the  $\pm$  fixes the direction of wave propagation relative to current.  $-U$  denotes wave propagation against current.  $+U$  denotes wave propagation with current. Using this convention, waves in both directions of current will have positive wavenumbers.  $n = 1$  and  $n = 2$  correspond to “small” (type I) and “large” (type II) wavenumber solutions respectively. Type II modes have no analogy for plane wave dispersion in a *locally* comoving frame [Peregrine and Jonsson, 1983]. The four non-trivial wave mode solutions from (14) are listed explicitly in Table (1).

### 3 Geometric demonstration of resonance

*Existence* of resonance conditions for water waves on uniform current is demonstrated geometrically using the description for a laboratory observer (absolute frequencies). Resonance occurs from a “tuning” of

<sup>4</sup>An alternative convention, which defines antiparallel nontrivial wave modes by oppositely signed wavenumbers, is also possible. The two conventions and their equivalence are discussed in Appendix B.

the wave field by dispersion. When a system is in resonance, phases of linear and nonlinear components match. This causes secular growth of nonlinear terms [Phillips, 1960]. The triad resonance condition is [cf. Hammack and Henderson, 1993]

$$\omega_a + \omega_b - \omega_c = 0, \quad (16)$$

$$k_a + k_b - k_c = 0. \quad (17)$$

A resonance *exists* if (16) and (17) can be satisfied along with the dispersion relation. Deriving resonance conditions is often algebraically tedious. However, *existence* of resonance may be easily and unambiguously demonstrated graphically. The graphical approach involves finding intersections between solution curves of (16) and (17) when constrained by the dispersion relation. The approach has been used to demonstrate resonances involving internal waves [Ball, 1964], gravity-capillary waves [Simmons, 1969], and vorticity waves [Drivas and Wunsch, 2015].

The procedure is as follows: first, plot the solution curve of a dispersion relation  $D_1(k, \omega)$  with its origin at  $O_1 = (0, 0)$ . Second, plot the solution curve again with its origin at  $O_2 = (k_a, \omega_a)$ , wherein  $(k_a, \omega_a)$  is a solution of  $D_1$  (i.e.  $D_2(k_a, \omega_a)$  wherein  $(k_a, \omega_a) \in \mathbb{R}^+ | D_1(k, \omega) = 0$ ). If there is a point of intersection between  $D_1$  and  $D_2$ , it represents a solution to the vector equation

$$\begin{Bmatrix} \omega_a \\ k_a \end{Bmatrix} + \begin{Bmatrix} \omega_b \\ k_b \end{Bmatrix} = \begin{Bmatrix} \omega_c \\ k_c \end{Bmatrix}. \quad (18)$$

Since this solution falls on both solution curves of the dispersion relation, it is equivalent to solving the algebraic system given by (16) and (17) along with the constraint of dispersion. Accordingly, it represents the *existence* of a triad resonance.

In figures 2a-2d, the procedure is applied to the wave-current dispersion relation in the form given by (13). In figure 2a the solution curve for  $D_1(k, \omega, -U)$  is plotted. In figure 2b, the solution curve for  $D_2(k, \omega, U)$  is plotted along  $D_1$ . They are seen to intersect at a point  $O_3$ . This demonstrates the *existence* of a triad resonance for deep water gravity waves propagating in opposite directions on uniform current. Resonant wavenumbers and frequencies are given by  $\overline{O_1 O_2}$ ,  $\overline{O_2 O_3}$  and  $\overline{O_1 O_3}$  (see figure 2c). The graphical solution simplifies to a vector representation (see figure 2d) which represents a solution to (18). Since the closure is in terms of absolute frequencies, it represents a resonant condition for a laboratory observer. The *existence* of nontrivial deep water gravity wave triad resonances on uniform current is the main finding of this paper.

## 4 Resonance conditions for a laboratory observer

A laboratory observer sees the fluid move with the current velocity,  $U$ , and measures absolute frequencies,  $\omega$ . Consider three plane waves:  $a_m, a_p^-$  and  $a_r$ .  $a_m$  and  $a_r$  propagate with current, and  $a_p^-$  propagates against current. Introduce (15) into (16) and (17). The triad closure for a laboratory observer is

$$\omega_m + \omega_p - \omega_r = 0, \quad (19)$$

$$k_{mn}^\pm + k_{pq}^\pm - k_{rs}^\pm = 0. \quad (20)$$

The velocity potential is

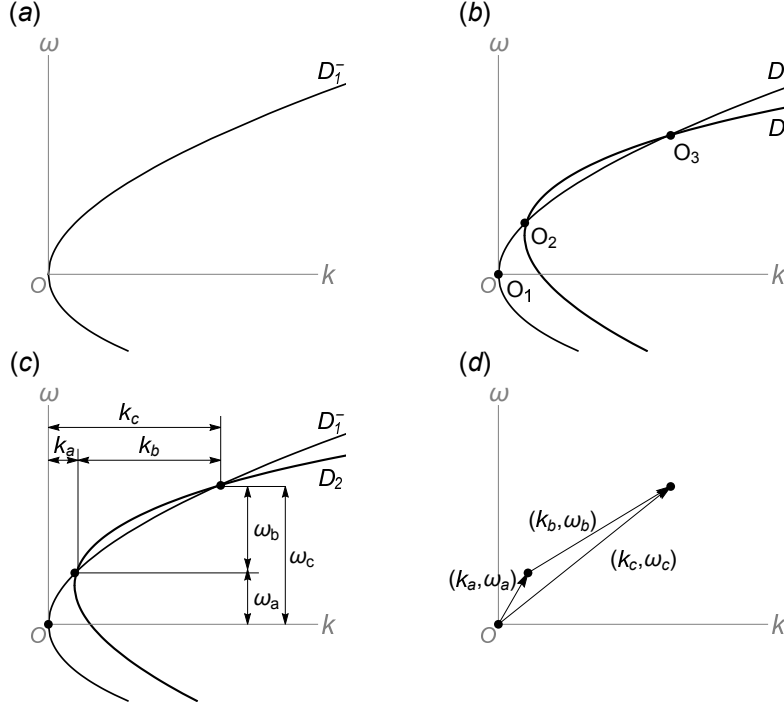


Figure 2: *Existence* of resonance for antiparallel gravity waves on uniform current is demonstrated graphically. (a) First, plot  $D_1(k, \omega, -U) = \omega = -kU + \sqrt{g|k|}$  with origin at  $O_1 = (k, \omega) = (0, 0)$ . (b) Second, plot  $D_2(k, \omega, U) = \omega = kU + \sqrt{g|k|}$  with origin at  $O_2 = (k_a, \omega_a)$ , wherein  $(k_a, \omega_a)$  is a solution of  $D_1(k, \omega, -U)$ . Intersection of solution curves at point  $O_3$  represents the *existence* of resonance. (c) Resonant wavenumbers and frequencies are given by  $\overline{O_1O_2}$ ,  $\overline{O_2O_3}$  and  $\overline{O_1O_3}$ . (d) Graphical solution reduces to vector representation of resonance closure.

$$\begin{aligned}\tilde{\phi} = & \left\{ b_{mn} e^{k_{mn} z} e^{i\theta_{mn}} + c.c. \right\} + \left\{ b_{pq}^- e^{k_{pq}^- z} e^{i\theta_{pq}} + c.c. \right\} \\ & + \left\{ b_{rs} C_{rs} e^{k_{rs} z} e^{i\theta_{rs}} + c.c. \right\}.\end{aligned}\quad (21)$$

Wherein,  $b = (c - U)a$  and  $\theta = kx - \omega t$ . The first permutation refers to absolute frequency and the second permutation denotes type I or type II wavenumber modes (see §2.2). Linear evolution is given by (10).

$$\mathcal{L}(\tilde{\phi}) = \frac{\partial^2 \tilde{\phi}}{\partial t^2} + g \frac{\partial \tilde{\phi}}{\partial z} + 2U \frac{\partial^2 \tilde{\phi}}{\partial x \partial t} + U^2 \frac{\partial^2 \tilde{\phi}}{\partial x^2}, \quad z = 0. \quad (22)$$

The three-wave system in matrix form is

$$\mathbf{M}b = 0. \quad (23)$$

Wherein,  $\mathbf{M}$  is a matrix of coefficients and  $b$  is a vector of amplitudes. Assuming (21), the coefficients have the form

$$\mathcal{D}(k_{mn}, \omega_m, U) = U^2 k_{mn}^2 + (-2U\omega_m - g)k_{mn} + \omega_m^2 = 0. \quad (24)$$

Combining (23) and (24) yields

$$\begin{bmatrix} \mathcal{D}_m(k_{mn}, \omega_m, U) & 0 & 0 \\ 0 & \mathcal{D}_p(k_{pq}^-, \omega_p, -U) & 0 \\ 0 & 0 & \mathcal{D}_r(k_{rs}, \omega_r, U) \end{bmatrix} \begin{bmatrix} b_{mn} \\ b_{pq}^- \\ b_{rs} \end{bmatrix} = \begin{bmatrix} 0 \\ 0 \\ 0 \end{bmatrix}. \quad (25)$$

A vanishing determinant yields the eigenvalues of the system

$$\left( (\omega_m - k_{mn}U)^2 - gk_{mn} \right) \left( (\omega_p + k_{pq}^-U)^2 - gk_{pq}^- \right) \left( (\omega_r - k_{rs}U)^2 - gk_{rs} \right) = 0. \quad (26)$$

This produces three dispersion relations

$$\omega_m - k_{mn}U = \sqrt{gk_{mn}}, \quad (27)$$

$$\omega_p + k_{pq}^-U = \sqrt{gk_{pq}^-},$$

$$\omega_r - k_{rs}U = \sqrt{gk_{rs}}. \quad (28)$$

Seek a solution of (27)-(28) which also satisfies the constraints of a triad resonance,

$$\omega_m + \omega_p = \omega_r, \quad (29)$$

$$k_{mn} + k_{pq}^- = k_{rs}. \quad (30)$$

Recall, a positive wavenumber number convention has been chosen. Introduce the scaling



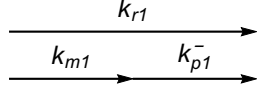
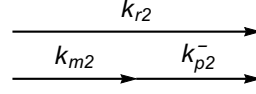
**(a) Type I modes (n=1)****(b) Type II modes (n=2)**

Figure 3: Resonant wavenumber schematic: antiparallel waves (with respect to current direction) may resonate on uniform current in deep water. – superscript denotes wave against current. Subscripts  $m, p, r$  denote frequencies which satisfy  $\omega_m + \omega_p = \omega_r$ . Second subscript denotes wavenumber type. For resonance, all modes must be either type I or II.

$$\omega_p \rightarrow \mu \omega_m, \quad \omega_r \rightarrow (1 + \mu) \omega_m. \quad (31)$$

The resonance condition becomes

$$\omega_m + \mu \omega_m = (1 + \mu) \omega_m, \quad (32)$$

$$k_{mn} + k_{pq}^- = k_{rs}. \quad (33)$$

$\mu$  is the ratio between initial harmonics. A self-interaction, an interaction between two waves with same frequency, is given by  $\mu = 1$ . Increasing  $\mu$  gives resonance for a higher upstream harmonic. Combine (26) and (31), and solve for wavenumbers. This yields

$$k_{mn} = \frac{g + 2U\omega_m + (-1)^n \sqrt{g(g + 4U\omega_m)}}{2U^2}, \quad (34)$$

$$k_{pq}^- = \frac{g - 2\mu U\omega_m + (-1)^n \sqrt{g(g - 4\mu U\omega_m)}}{2U^2}, \quad (35)$$

$$k_{rs} = \frac{g + 2(\mu + 1)U\omega_m + (-1)^n \sqrt{g(g + 4(\mu + 1)U\omega_m)}}{2U^2}. \quad (36)$$

If all modes are either type I or II modes ( $n = q = s$ ), nontrivial solutions for (34)-(36) and (33) exist. Figure 3 gives a schematic of resonant combinations.

Resonance conditions reduce to a relationship between  $\omega_m$  and  $\mu$ . Before satisfying the final constraint, (33), it is convenient to switch to non-dimensional forms,

$$w = \omega \frac{U}{g}, \quad \kappa = k \frac{U^2}{g}. \quad (37)$$

The resonance closure becomes

$$w_{mn} + \mu w_{mn} - (1 + \mu) w_{mn} = 0, \quad (38)$$

$$\kappa_{mn} + \kappa_{pq}^- - \kappa_{rs} = 0. \quad (39)$$

Wavenumber solutions are

Type I modes (n = 1)						Type II modes (n = 2)					
$\mu$	.2	.4	.6	.8	1	$\mu$	.2	.4	.6	.8	1
$w_{m1} = \frac{\omega U}{g}$	1.170	.545	.339	.238	.178	$w_{m2} = \frac{\omega U}{g}$	1.122	.599	.395	.295	.235

Table 2: Deep water gravity wave triad resonance conditions reduce to universal constants of non-dimensional parameter  $w_{mn}$ . Resonance closure is  $\omega_m + \mu\omega_n = (1 + \mu)\omega_s$ ,  $k_{mn} + k_{pq}^- = k_{rs}$ . All modes must be type I or type II,  $n = q = s$ .  $\mu$  is ratio of initial harmonics.

$$\kappa_{mn} = \frac{1}{2} (1 + 2w_{mn} + (-1)^n \sqrt{4w_{mn} + 1}), \quad (40)$$

$$\kappa_{pq}^- = \kappa_{pn}^- = \frac{1}{2} (1 - 2w_{mn}\mu + (-1)^n \sqrt{1 - 4w_{mn}\mu}), \quad (41)$$

$$\kappa_{rs} = \kappa_{rn} = \frac{1}{2} (1 + 2w_{mn} (1 + \mu) + (-1)^n \sqrt{4w_{mn} (1 + \mu) + 1}). \quad (42)$$

Equation (39) and (40)-(42) reduce to

$$4\mu w_{mn} + \sqrt{1 - 4\mu w_{mn}} + \sqrt{4w_{mn} + 1} = \sqrt{4(\mu + 1)w_{mn} + 1} + 1. \quad (43)$$

Exact solution of (43) is given in Appendix E. If  $\mu$  is known a priori, resonance conditions reduce to universal constants. Some values are given in Table 2. Resonant frequency and wavenumber solution curves are shown in figure 4. For Type I modes, a greater difference in initial harmonics (larger  $\mu$ ) resonates lower frequencies and wavenumbers (see figs. 4a-b). Similar behavior is seen for type II mode resonant frequencies (see fig. 4c). In contrast to the type I mode case, resonant upstream wavenumbers are greater for type II modes (see fig. 4d).

#### 4.1 Example: Self-interactions for absolute frequencies

Consider a self-interaction ( $\mu = 1$ ) between type I modes ( $n = 1$ ). The resonance condition, (43), is

$$w_{m1} \approx .178. \quad (44)$$

The exact form is given in Appendix E.  $\kappa$ -values follow from (40)-(42). Resonant frequencies and wavenumbers are

$$w_{m1} \approx .178, \quad w_{p1} \approx .178, \quad w_{r1} \approx .356, \quad (45)$$

$$\kappa_{m1} \approx .024, \quad \kappa_{p1}^- \approx .054, \quad \kappa_{r1} \approx .078. \quad (46)$$

Similarly, for type II modes ( $n = 2$ ) and self-interactions ( $\mu = 1$ ),

$$w_{m2} \approx .235. \quad (47)$$

Resonant values are

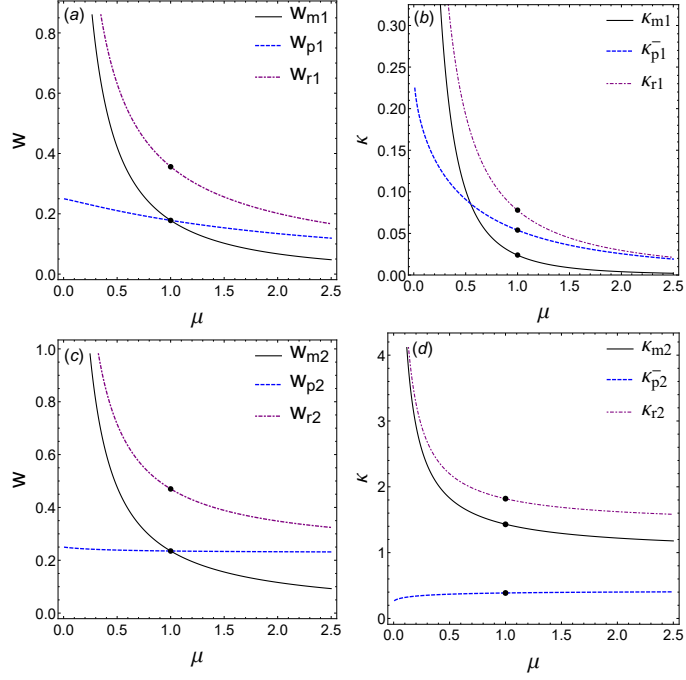


Figure 4: Resonance solution curves for a laboratory viewer. The second permutations,  $n = 1$  and  $n = 2$ , correspond to type I and II wavenumber modes. (a) Type I mode resonant frequencies: larger difference between initial harmonics (larger  $\mu$ ) generates slower waves (lower frequencies); purple-dot dashed line. (b) Resonant type I wavenumbers: increasing  $\mu$  generates longer upstream waves (smaller wavenumbers). (c) Type II mode resonant frequencies: larger difference between initial harmonics (larger  $\mu$ ) generates lower frequencies. (d) Resonant type II wavenumbers: increasing  $\mu$  generates longer waves. Black dots mark resonant values for special case of a self-interaction ( $\mu = 1$ ).

$ U $	Type I					Type II				
	$\omega_{m1} = \omega_{p1}^-$	$\omega_{r1}$	$k_{m1}$	$k_{p1}^-$	$k_{r1}$	$\omega_{m2} = \omega_{p2}^-$	$\omega_{r2}$	$k_{m2}$	$k_{p2}^-$	$k_{r2}$
.5	3.49	6.98	.94	2.12	3.10	4.61	9.21	56.06	15.29	71.34
1	1.74	3.49	.24	.53	.76	2.30	4.61	14.01	3.82	17.84
1.5	1.16	2.33	.10	.24	.34	1.54	3.07	6.23	1.70	7.93
2	.87	1.74	.06	.13	.19	1.15	2.30	3.50	.96	4.59

Table 3: Dimensional values which satisfy self-interaction resonance conditions as observed by a laboratory viewer. Self-interactions satisfy universal values of non-dimensional parameters,  $\{\kappa_{m1}, \kappa_{p1}^-, \kappa_{r1}, w_m\} \approx \{.024, .054, .078, .178\}$  and  $\{\kappa_{m2}, \kappa_{p2}^-, \kappa_{r2}, w_m\} \approx \{1.43, .387, 1.82, .235\}$  for type I and II modes respectively. Generally speaking, faster currents resonate lower frequencies (longer waves). The gravity wave regime is most affected. (Units:  $U [\frac{m}{s}]$ ,  $k [\frac{rad}{m}]$  and  $\omega [\frac{rad}{s}]$  )

$$w_{m2} \approx .235, \quad w_{p2} \approx .235, \quad w_{r2} \approx .470, \quad (48)$$

$$\kappa_{m2} \approx 1.43, \quad \kappa_{p2}^- \approx .387, \quad \kappa_{r2} \approx 1.820. \quad (49)$$

Numerical values may be found algebraically using algebraic procedures or directly from the solution curves given in figure 4. Resonant values for the special case of self-interactions involving type I and II modes, given in (45)-(46) and (48)-(49) respectively, are marked in Fig. 4.

Dimensional parameters are easily recovered from the non-dimensional conditions. Some dimensional values are given in Table 3. Realistic current velocities mostly affect the gravity wave regime. Generally, faster currents resonate lower frequencies (longer waves) and slower currents resonate higher frequencies (shorter waves). The existence of two different resonant conditions suggests the dominant energy transfer mechanism will not be homogeneous across a wave spectrum. The non-dimensional parameter  $w = \omega U g^{-1}$  has been discussed for resonance between waves and an external forcing [cf. Dagan and Miloh, 1982, Tyvand and Torheim, 2012]. The above results suggest the parameter is also an indicator of an intrinsic energy sharing mechanism within wave-current fields.

## 5 Resonance for an observer moving with velocity $U$

In §4, resonance conditions were derived for a laboratory observer. It is tempting to assume, since applying a Galilean shift to a single plane wave yields the intrinsic frequency of that wave, uniform application of a Galilean shift to the resonance closure in a lab frame will recover the resonance closure in terms of intrinsic frequencies. This is not always true. Indeed, for the triad resonance between waves propagating in opposite directions with respect to current, discussed in section §4, it is false (see Appendix C). A rigorous transformation to a moving observer ought to derive the dispersion relations from the governing equations anew.

Define a second observer, moving with a velocity  $U'$ , who observes the resonant system discussed in §4. One may not assume *a priori* that this observer describes the system by three intrinsic frequencies (see Appendix C). Denote frequencies for this viewer by a yet to be defined frequency description:  $v$ -frequencies. The resonance closure in terms of  $v$ -frequencies is

$$v_m + v_p - v_r = 0, \quad (50)$$

$$k_m + k_p^- - k_r = 0. \quad (51)$$

It should be emphasized, the relationship between 50 and 20 is given by the dispersion relations which are not known *a priori*. The procedure of §4 may now be repeated. Dispersion relations are derived assuming periodicity, and resonance conditions are found by solving the system's determinant along with a constraint for resonant phase matching.

The linear operator, (10), used in §4, may be applied for the new observer. The evolution equation for each plane wave is now given by

$$\mathcal{L}(\tilde{\phi}) = \frac{\partial^2 \tilde{\phi}}{\partial t^2} + g \frac{\partial \tilde{\phi}}{\partial z} + 2V_{mn} \frac{\partial^2 \tilde{\phi}}{\partial x \partial t} + V_{mn}^2 \frac{\partial^2 \tilde{\phi}}{\partial x^2}, \quad z = 0. \quad (52)$$

Wherein,  $V_{mn}$  is an effective current on each plane wave in the new description. It is found by addition of velocities,

$$V_{mn} = \pm U - U'.$$

If the velocity of the moving observer is the same sign and magnitude as current,  $U' = U$ . Then, for waves following current,  $V_{mn} = +U - U = 0$ . And, for the wave opposing the current,  $V_{mn}^- = -U - U = -2U$ . Thus, the two waves following current (and observer),  $a_{rs}$  and  $a_{mn}$ , will “feel” no effective current. Whereas, the wave opposing current (and observer),  $a_{pq}^-$ , will “feel” an ambient current due to the preferential direction of the media. Using these definitions for  $V_{mn}$ , one may now derive the correct dispersion relations from the governing equations. A less conceptual, but more mathematically transparent, derivation is given in Appendix C.

The three-wave system in matrix form is

$$\mathbf{M}b = 0. \quad (53)$$

Wherein,  $\mathbf{M}$  is a matrix of coefficients and  $b$  is a vector of velocity potential amplitudes. Assume spatial and temporal periodicity, the coefficients become

$$\mathcal{D}(k_{mn}, v_m, V_{mn}) = V_{mn}^2 k_{mn}^2 + (-2V_{mn}v_m - g)k_{mn} + v_m^2 = 0. \quad (54)$$

Combine (53) and (54) with appropriate definitions of  $V$ ,

$$\begin{bmatrix} \mathcal{D}_m(k_{mn}, v_m, 0) & 0 & 0 \\ 0 & \mathcal{D}_p(k_{pq}^-, v_p, -2U) & 0 \\ 0 & 0 & \mathcal{D}_r(k_{rs}, v_r, 0) \end{bmatrix} \begin{bmatrix} b_{mn} \\ b_{pq} \\ b_{rs} \end{bmatrix} = \begin{bmatrix} 0 \\ 0 \\ 0 \end{bmatrix}. \quad (55)$$

Eigenvalues are found when the determinant of (55) vanishes,

$$(v_m^2 - gk_{mn}) \left( (v_p + 2k_{pq}^- U)^2 - gk_{pq} \right) (v_r^2 - gk_{rs}) = 0. \quad (56)$$

This produces three dispersion relations

$$v_m = \sqrt{gk_m}, \quad (57)$$

$$v_p + 2k_p^- U = \sqrt{gk_p^-}, \quad (58)$$

$$v_r^2 = \sqrt{gk_r}. \quad (59)$$

Seek a solution of (57)-(59) which also satisfies the constraint of resonance,

$$v_m + \mu v_m - (1 + \mu) v_m = 0, \quad (60)$$

$$k_{mn} + k_{pq}^- - k_{rs} = 0. \quad (61)$$

Combine (56) and (60), taking into account the resonance requirement that  $n = q = s$ , yields the wavenumbers,

$$k_{mn} = \frac{v_m^2}{g}, \quad (62)$$

$$k_{pq}^- = k_{pn}^- = \frac{g - 4\mu U v_m + (-1)^n \sqrt{g(g - 8\mu U v_m)}}{8U^2}, \quad (63)$$

$$k_{rs} = k_{rn} = \frac{(\mu + 1)^2 v_m^2}{g}. \quad (64)$$

The dispersion relations for the two waves propagating with the current, (62) and (64), are single valued functions. Whereas, the dispersion relation for the plane wave propagating against the current, (63), is multi-valued. It is of interest to note, the third term in (63) gives the wave-blocking condition,  $g - 8\mu U v_m = 0$ ,

$$\frac{U v_m}{g} > \frac{1}{8\mu}. \quad (65)$$

Noting  $U = v/2$  recovers the known blocking condition  $\sim 1/4$ . Nontrivial solutions to (61) and (62)-(64) are found when all modes are either type I or type II ( $n = q = s$ ). Note, the second permutation is retained for all waves even when their dispersion form has one solution. Non-dimensionalization shows all solutions are implicitly dependent on the permutation  $n$ . See figure 3b for a schematic of resonant wavenumber combinations. Before satisfying (61), introduce non-dimensional parameters

$$v = v \frac{U}{g}, \quad \kappa = k \frac{U^2}{g}. \quad (66)$$

Wavenumber solutions become

$$\kappa_{mn} = v_m^2, \quad (67)$$

$$\kappa_{pq}^- = k_{pn}^- = \frac{1}{8} \left( 1 - 4\mu v_m + (-1)^n \sqrt{1 - 8\mu v_m} \right), \quad (68)$$

$$\kappa_{rs} = \kappa_{rn} = (\mu + 1)^2 v_m^2. \quad (69)$$

Equations (67)-(69) and (61) reduce to

$$\frac{1}{8} \left( 1 + (-1)^n \sqrt{1 - 8\mu v_{mn}} - 4\mu v_{mn} (1 + 2(\mu + 2)v_{mn}) \right) = 0. \quad (70)$$

Equation (70) has an exact solution when

$$v_{mn} = \left( \mu(\mu + 2) + (-1)^{n+1} \sqrt{\mu(\mu + 2)^3} \right)^{-1}. \quad (71)$$

Substitute (71) into (62)-(64). Resonant wavenumbers are

$$\kappa_{mn} = \frac{1}{\left( \mu(\mu + 2) + (-1)^{n+1} \sqrt{\mu(\mu + 2)^3} \right)^2}, \quad (72)$$

$$\begin{aligned} \kappa_{pn}^- = \frac{1}{8} \left( 1 - \frac{4\mu}{\mu(\mu + 2) + (-1)^{n+1} \sqrt{\mu(\mu + 2)^3}} \right. \\ \left. + (-1)^n \sqrt{1 - \frac{8\mu}{\mu(\mu + 2) + (-1)^{n+1} \sqrt{\mu(\mu + 2)^3}}} \right), \end{aligned} \quad (73)$$

$$\kappa_{rn} = \frac{(\mu + 1)^2}{\left( \mu(\mu + 2) + (-1)^{n+1} \sqrt{\mu(\mu + 2)^3} \right)^2}. \quad (74)$$

When  $n = 1$ , (73) gives the wave-blocking condition in  $\mu$ -space. The blocking point occurs when

$$1 - \frac{8\mu}{\mu(\mu + 2) + \sqrt{\mu(\mu + 2)^3}} = 0.$$

This corresponds to

$$\mu = \frac{2}{3}. \quad (75)$$

The  $v$ -description is more analytically tractable than the laboratory frame (compare (71) with Appendix E). Thus, it is more convenient for analysis. Solution curves for resonant values measured by the moving observer are given in figure 5. Resonant type I frequencies are positive and decrease with  $\mu$  (see fig. 5a). The solution curve for resonant type I wavenumbers exhibits an inflection point at the wave-blocking condition  $\mu = 2/3$  (see fig. 5b). The inflection point occurs for the upstream wave. For type II modes, the resonant frequencies are negative (see fig. 5c). A greater difference between initial harmonics (larger  $\mu$ ) generates longer waves (see fig. 5d).

## 5.1 Example: Self-interactions

For a self-interaction,  $\mu = 1$  in (71) and

$$v_{mn} = \left( 3 - (-1)^n 3\sqrt{3} \right)^{-1}. \quad (76)$$

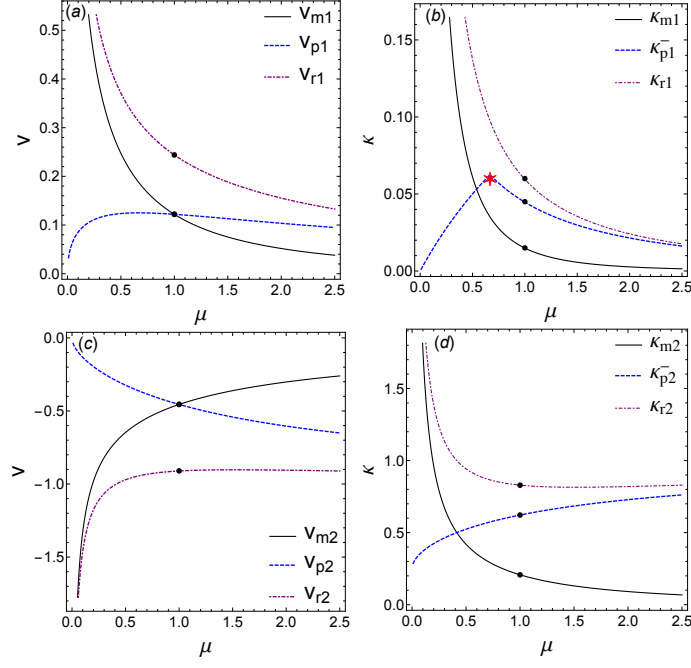


Figure 5: Resonant solution curves for antiparallel waves seen by an observer moving with the current velocity  $U$ . The second permutations,  $n = 1$  and  $n = 2$ , correspond to type I and II wavenumber modes. (a) Type I mode resonant frequencies: larger difference in initial harmonics (larger  $\mu$ ) generates lower frequencies, purple-dot dashed line. (b) Resonant type I wavenumbers: increasing  $\mu$  generates long waves (lower wavenumbers). Effect of wave-blocking on resonances seen at inflection point; red star, of upstream wave solution curve; blue-dashed line. (c) Type II mode resonant frequencies: larger  $\mu$  generates smaller negative frequencies. (d) Resonant type II wavenumbers: increasing  $\mu$  generates longer waves. Black dots mark resonant values for special case of a self-interaction ( $\mu = 1$ ).



Consider a self-interaction between type I modes ( $n = 1$ ), (76) yields

$$v_{n1} = \left(3 + 3\sqrt{3}\right)^{-1} \approx .122. \quad (77)$$

Equations (72)-(74) give resonant  $\kappa$ -values. Resonance values are

$$v_{m1} \approx .122, \quad v_{p1} \approx .122, \quad v_{r1} \approx .244, \quad (78)$$

$$\kappa_{m1} \approx .015 \quad \kappa_{p1}^- \approx .045, \quad \kappa_{r1} \approx .060. \quad (79)$$

Similarly, for type II modes ( $n = 2$ ) and self-interactions ( $\mu = 1$ ),

$$v_{n2} = \left(3 - 3\sqrt{3}\right)^{-1} \approx -.455. \quad (80)$$

Resonant values are

$$v_{m2} \approx -.455, \quad v_{p2} \approx -.455, \quad v_{r2} \approx -.910, \quad (81)$$

$$\kappa_{m2} \approx .207 \quad \kappa_{p2}^- \approx .622, \quad \kappa_{r2} \approx .829. \quad (82)$$

Numerical values may be found algebraically or directly from the solution curves given in figure 5. Resonant values for the special case of self-interactions involving type I and II modes, given in (78)-(79) and (81)-(82) respectively, are marked by black dots in Fig. 5.

## 6 Amplitude coupling

Growth due to resonant phase matching is known to be arrested by amplitude coupling [Benney, 1962]. Nonetheless, if the interaction time is sufficiently long, nonlinear terms may still grow to first-order magnitude. In this section, a three-wave interaction model for surface amplitudes is adapted for a resonant wave-current system involving waves propagating in both directions with respect to current.

It was discussed in §5 that a viewer moving with a velocity  $U$ , who will see the fluid “still,” will not describe the system of waves propagating in opposite directions with respect to current, given in §4, by three intrinsic frequencies (see also Appendix 135). Rather, this observer sees frequencies given by the dispersion relations (57)-(59). Incorporating the definitions of the intrinsic frequency,  $\sigma_i = \sqrt{gk_i}$  into these dispersion relations yields

$$v_m = \sigma_m, \quad (83)$$

$$v_p = \sigma_p - 2k_p^- U, \quad (84)$$

$$v_r = \sigma_r. \quad (85)$$

Thus,  $v$ -frequencies may be understood to be the intrinsic frequencies of the original system transformed in such a way that the mode propagating against current has a correction due to the preferential direction of the media. As such, it is the  $v$ -description, not the  $\sigma$ -description, which consistently describe a system

of waves propagating on both directions with respect to current for a viewer who moves with the velo. Accordingly, the transformations given by (83)-(85), may be incorporated into a three-wave interaction model for a viewer which sees still water.

A coupled three-wave model for a viewer who sees surface water waves propagating on “still” water is of the form

$$\frac{da_r}{d\tau} = \beta^{(1)} a_m a_p, \quad \frac{da_m}{d\tau} = -\beta^{(2)} a_p a_r, \quad \frac{da_p}{d\tau} = -\beta^{(3)} a_m a_r. \quad (86)$$

Wherein, the nonlinear coefficients are

$$\beta^{(1)} = \frac{k_r v_m v_p}{4v_r^2} \left( \frac{k_m v_r^2}{k_r v_p} + \frac{k_p v_r^2}{k_r v_m} - \frac{v_m^2}{v_p} - \frac{v_p^2}{v_m} \right), \quad (87)$$

$$\beta^{(2)} = \frac{k_m v_p v_r}{4v_m^2} \left( \frac{k_r v_m^2}{k_m v_p} - \frac{k_p v_m^2}{k_m v_r} - \frac{v_r^2}{v_p} + \frac{v_p^2}{v_r} + 4v_r \right), \quad (88)$$

$$\beta^{(3)} = \frac{k_p v_m v_r}{4v_p^2} \left( -\frac{k_m v_p^2}{k_p v_r} + \frac{k_r v_p^2}{k_p v_m} + \frac{v_m^2}{v_r} - \frac{v_r^2}{v_m} + 4v_p \right). \quad (89)$$

The reader is referred to McGoldrick [1965] for the original derivation. The above form is reduced for the case of waves without capillary effects. In contrast to the original formulation, it is written in terms of  $v$ -frequencies which are  $\sigma$ -frequencies with a correction for wave motion in both directions with respect to current.

Introduce non-dimensional parameters

$$v_{mn} = \frac{v_m U}{g}, \quad \kappa_{mn} = \frac{k_{mn} U^2}{g}, \quad \tau = v_{ref} t, \quad A_{mn} = k_{ref} a_{mn}. \quad (90)$$

$v_{ref}$  and  $k_{ref}$  are the frequency and wavenumber of the initial component following current. The system may be written as

$$\frac{dA_{rn}}{d\tau} = B^{(mp)} A_{mn} A_{pq}^-, \quad \frac{dA_{mn}}{d\tau} = -B^{(pr)} A_{pq}^- A_{rs}, \quad \frac{dA_{pq}^-}{d\tau} = -B^{(mr)} A_{mn} A_{rs}. \quad (91)$$

Nonlinear coefficients are

$$B^{(mp)} = \frac{\kappa_{rs} v_{mn} v_{pq}}{4v_{rs}^2} \left( \frac{v_{rs}^2}{\kappa_{rs} v_{mn} v_{pq}} + \frac{\kappa_{pq} v_{rs}^2}{\kappa_{rs} \kappa_{mn} v_{mn}^2} - \frac{v_{mn}}{\kappa_{mn} v_{pq}} - \frac{v_{pq}^2}{\kappa_{mn} v_{mn}^2} \right), \quad (92)$$

$$B^{(pr)} = \frac{\kappa_{mn} v_{rs} v_{pq}}{4v_{mn}^2} \left( \frac{v_{mn}^2 \kappa_{rs}}{v_{pq}^2 \kappa_{mn} \kappa_{pq}} - \frac{v_{mn}^2}{v_{rs} \kappa_{mn} v_{pq}} - \frac{v_{rs}^2}{v_{pq}^2 \kappa_{pq}} + \frac{v_{pq}}{v_{rs} \kappa_{pq}} + \frac{4v_{rs}}{v_{pq} \kappa_{pq}} \right), \quad (93)$$

$$B^{(mr)} = \frac{\kappa_{pq} v_{mn} v_{rs}}{4v_{pq}^2} \left( -\frac{\kappa_{mn}}{\kappa_{pq} \kappa_{rs} v_{rs}^2} + \frac{v_{pq}^2}{\kappa_{pq} v_{mn} v_{rs}} + \frac{v_{mn}^2}{\kappa_{rs} v_{rs}^2} - \frac{v_{rs}}{\kappa_{rs} v_{mn}} + \frac{4v_{pq}^2}{v_{pq} \kappa_{rs} v_{rs}} \right). \quad (94)$$

For resonant waves ( $n = q = s$ ), wavenumbers are given by (72)-(74). Equations (92)-(94) become

$$B_n^{(mp)} = \frac{1}{32v_{mn}^2} \left( (1 + (-1)^n R_{mn}) \mu - 4v_{mn} \mu^2 - 8v_{mn}^2 \mu^3 \right), \quad (95)$$

$$B_n^{(pr)} = -\frac{1}{4} + \frac{2v_{mn}^2 (4 + 8\mu + 5\mu^2)}{1 + (-1)^n R_{mn} - 4v_{mn} \mu}, \quad (96)$$

$$B_n^{(mr)} = \frac{1}{32\mu^2(\mu+1)v_{mn}^2} \left( (1 + (-1)^n + (1 + (-1)^n R_{mn} - 4v) \mu + (-1)^n R_{mn} + 24v_{mn}^2 - 4v_{mn} - 1) \mu^2 + (24v_{mn}^2 + 4v_{mn}) \mu^3 + 8v_{mn}^2 \mu^4 \right). \quad (97)$$

Wherein,

$$R_{mn} = \sqrt{1 - 8\mu v_{mn}}.$$

Equations (95)-(97) depend only on  $\mu$ ,  $v$  and permutation  $n$ . However,  $v$  is also expressible as a function solely of  $\mu$  through (71). Accordingly, nonlinear coefficients have been written solely as a function of  $\mu$  and the permutation  $n$ , i.e.  $B_n^{(mp)} = B_n^{(mp)}(\mu)$ .

A solution to the system is known in terms of Jacobi-Elliptic functions (see McGoldrick, 1965, Alam et al., 2010). Define initial amplitudes:  $A_{mn}(0) = \hat{A}_{mn} \neq 0$ ,  $A_{pn}^-(0) = \hat{A}_{pn}^- \neq 0$  and  $A_{rn}(0) = 0$ . Let  $\alpha$  be a ratio of the initial upstream and downstream amplitudes,  $\alpha_n = \hat{A}_{pn}^- / \hat{A}_{mn}$ . The solution is governed by the parameter

$$m_n = \frac{B_n^{(pr)} \left( \hat{A}_{pn}^- \right)^2}{B_n^{(mr)} \hat{A}_{mn}^2}. \quad (98)$$

The dependency of  $m_n$  on  $\mu$  and initial amplitudes is shown in figure 6.

There are two solution cases. First,  $m_n \leq 1$ , the resonant amplitude is

$$A_{rn}(\tau) = \hat{A}_{pn}^- \left( \frac{B_n^{(mp)}}{B_n^{(mr)}} \right)^{1/2} \text{sn}(\chi_n | m_n). \quad (99)$$

Wherein,  $\chi_n = \hat{A}_{mn}^2 \left( B_n^{(mp)} B_n^{(mr)} \right)^{1/2} (\tau - \tau_0)$ . The initial waves evolve as

$$A_{mn}(\tau) = \hat{A}_{mn} \text{dn}(\chi_n | m_n), \quad (100)$$

$$A_{pn}^-(\tau) = \hat{A}_{pn}^- \text{cn}(\chi_n | m_n). \quad (101)$$

The second case is  $m_n > 1$ , the resonant amplitude is

$$A_{rn}(\tau) = \hat{A}_{mn} \left( \frac{B_n^{(mp)}}{B_n^{(pr)}} \right)^{1/2} \text{sn}(\chi_n | m_n^{-1}). \quad (102)$$

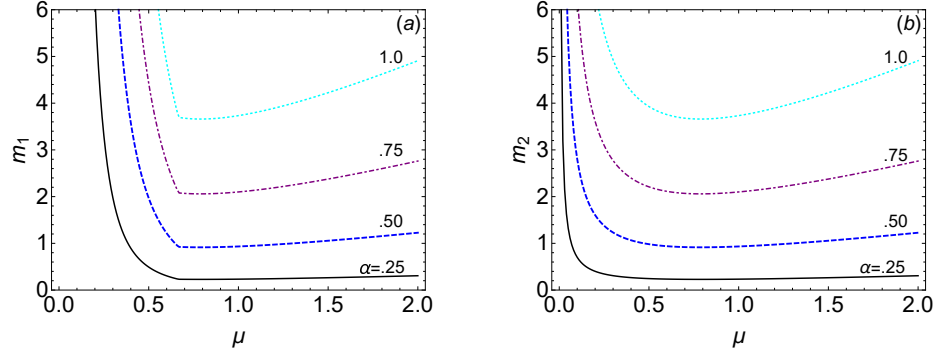


Figure 6: Effect of  $\mu$  on parameter  $m$ . Various initial conditions of  $\alpha = \hat{A}_{p1}/\hat{A}_{m1}$  shown for (a) type I modes and (b) type II modes. When  $m \leq 1$ , the  $\kappa_{pq}^-$  mode transfers energy to the generated wave at a faster rate than the  $\kappa_{mn}$  mode. When  $m > 1$ , the roles are reversed. The  $\kappa_{mn}$  mode transfers energy to the generated wave at a faster rate than the  $\kappa_{pq}$  mode. For  $\mu < 2/3$ ,  $m \leq 1$  for type I modes but  $m > 1$  for type II modes. In this regime, energy will be transferred more effectively from different directions on different wavenumber scales. The upper bound of this regime,  $\mu = 2/3$ , corresponds to the blocking point (see (75)).

Wherein,  $\chi_n = \left(\hat{A}_{pn}^-\right)^2 \left(B_n^{(mp)} B_n^{(pr)}\right)^{1/2} (\tau - \tau_0)$ . The initial waves evolve as

$$A_{mn}(\tau) = \hat{A}_{mn} \text{cn}(\chi_n | m_n^{-1}), \quad (103)$$

$$A_{pn}^-(\tau) = \hat{A}_{pn}^- \text{dn}(\chi_n | m_n^{-1}). \quad (104)$$

Solutions given by (99)-(104) represent a system wherein energy is shifted periodically between the three waves. The model demonstrates the most salient features of resonance: wave generation and cyclical amplitude coupling.

Figure 7 shows maximum resonant amplitudes and coupling for type I mode self-interactions. It is shown that increasing  $\mu$  and  $\alpha$  corresponds to higher harmonic interactions and greater initial downstream energy respectively. In the absence of other effects (i.e. wavebreaking and viscous dissipation) resonant amplitude increases for greater difference between harmonic interactions and greater initial downstream amplitude (see figure 7a). In figure 7b resonant cyclical energy exchange is shown for a self-interaction ( $\mu = 1$ ) with initial amplitudes  $\alpha = \hat{A}_{p1}/\hat{A}_{m1} = .5$ . Initial energy on the  $\kappa_{m1}$  and  $\kappa_{p1}^-$  modes is transferred to the  $\kappa_{r1}$  mode which is generated from zero.

Figure 8 shows maximum resonant amplitudes and coupling for type II self-interactions. In the absence of other effects, maximum amplitudes increase for higher harmonic interactions (larger  $\mu$ ) and for increasing initial downstream amplitude (larger  $\alpha$ ) (see figure 8a). Figure 8b shows cyclical exchange of energy due to amplitude coupling for a self-interaction and  $\alpha = \hat{A}_{p2}/\hat{A}_{m2} = .7$ . Initial energy on the  $\kappa_{m2}$  and  $\kappa_{p2}^-$  modes is transferred to the  $\kappa_{r2}$  mode which is generated from zero.

Different coupling behaviors may be observed on the wavenumber scales characteristic of type I and II modes. First, the strength and speed of the resonant interactions may vary for a given energy distribution across the wavenumber spectrum (compare figs. 7 and 8). Second, either the initial downstream wave (for example, figure 7b) or upstream wave (for example, figure 8b) may cycle through zero. These behaviors are governed by the parameter  $m_n$  which is a function of relative initial amplitudes.

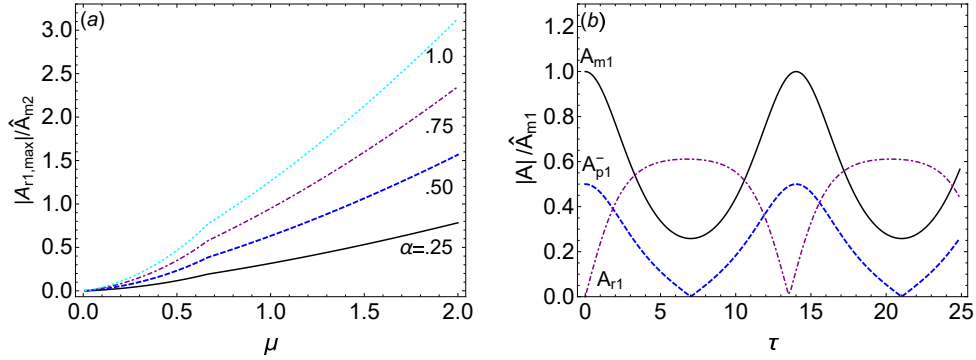


Figure 7: Type I mode resonance for observing moving with current (a) Resonant amplitude as function of  $\mu$  (ratio of initial harmonics) for various  $\alpha = \hat{A}_{p1}/\hat{A}_{m1}$  (ratio of initial amplitudes). Special case of self-interaction,  $\mu = 1$ , shown for initial condition  $\alpha = .5$ . Relative maximum resonant amplitude is  $\approx .6$ ; purple dot-dashed line. (b) Time evolution of amplitudes: Initial downstream wave  $A_{m1}$ ; solid black line, resonates with upstream wave  $A_{p1}^-$ ; blue dashed line, and generates downstream wave  $A_{r1}$ ; purple dot-dashed line.  $A_{r1}$  reaches amplitude  $\approx .6$ . Since model parameter  $m_1 = .993 < 1$ , upstream wave transfers energy to generated wave more efficiently than  $A_{m1}$  ( $A_{p1}^-$  cycles through zero).

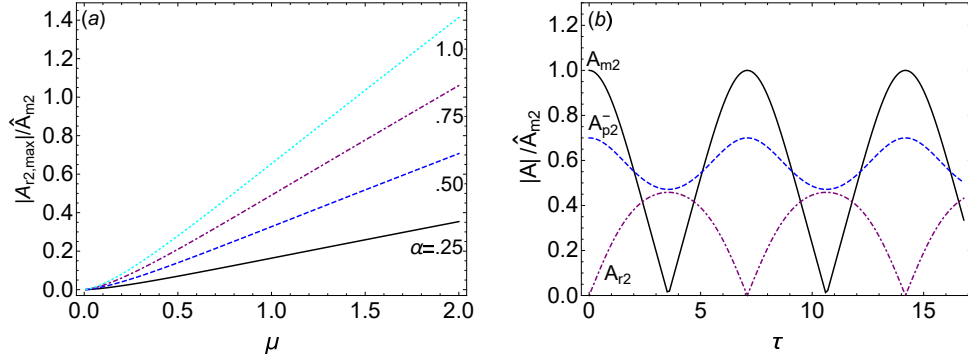


Figure 8: Type II mode resonance for an observer moving with current velocity: (a) Resonant amplitude as function of  $\mu$  (ratio of initial harmonics) for various  $\alpha = \hat{A}_{p2}/\hat{A}_{m2}$  (ratio of initial amplitudes). Consider a self-interaction,  $\mu = 1$ , and  $\alpha = .7$ . Relative maximum resonant amplitude is  $\approx .42$ ; purple-dashed line. (b) Time evolution of amplitudes: Initial downstream wave  $A_{m2}$ ; solid black line, resonates with upstream wave  $A_{p2}^-$ ; blue dashed line, and generates downstream wave  $A_{r2}$ ; purple dot-dashed line.  $A_{r2}$  reaches relative amplitude  $\approx .42$ . Since model parameter  $m_2 = 1.338 > 1$ , downstream wave transfers energy to generated wave more effectively than  $A_{p2}^-$  ( $A_{m2}$  cycles through zero).

$m_n$  is the effectiveness ratio of the initial waves in the energy transfer mechanism (see fig. 6). When  $m_n \leq 1$  the upstream mode,  $\kappa_{pn}^-$ , transfers energy to the resonant wave at a faster rate than  $\kappa_{mn}$ . As a result, the  $\kappa_{pn}^-$  mode cycles through zero. When  $m_n > 1$  the roles are reversed. The downstream mode,  $\kappa_{mn}$ , transfers energy to the resonant wave at a faster rate than  $\kappa_{pn}^-$ . In all cases  $m_n$  increases with increasing initial downstream wave amplitude,  $\hat{A}_{mn}$ . The regime  $\mu < 2/3$  is of particular interest, for example,  $\mu = .3$  and  $\alpha = .25$ . For these values, given the same amplitude ratio on both scales,  $m_n > 1$  for type I modes but  $m_n < 1$  for type II modes (compare figs. 6a and 6b). Energy will be more effectively transferred in different directions on different scales in wavenumber space. Namely, on the (smaller wavenumber) type I mode scale energy will be transferred more effectively by the downstream wave. Whereas, on the (larger wavenumber) type II mode scale, energy will be transferred more effectively by the upstream wave. For both mode types greater initial downstream energy (larger  $\alpha$ ) increases effectiveness of downstream energy transfer to the resonant wave. Realistically speaking, the energy distribution across wavenumber scales will not be linear and  $\alpha$  may be expected to vary between these scales.

Resonant behavior was seen to depend on wavenumber mode type and initial amplitudes. The second wavenumber type is produced by the modified dispersion relation (see §2.1). Initial relative amplitudes would depend on initial energy distribution as well as current velocity (cf. Longuet-Higgins and Stewart, 1960). Since the behavior varies between wavenumber scales (characterized by mode types), it represents a fundamental source of inhomogeneity. Inhomogeneities include speed and strength of resonance, and most effective direction of energy transfer. The resonances and inhomogeneities have no analogy without current, since the dispersion relation for this case will be single-valued and isotropic.

## 7 Conclusion

The main finding of this paper is the existence of new triad resonances for gravity waves propagating in opposite direction with respect to a uniform current. The triads are due to multivalued and anisotropic dispersion. They are a first of their kind for gravity waves in the sense that they are non-degenerate and occur without inhomogeneity even in deep water. They are produced by current *vis a vis* a modified dispersion relation. The most salient features of the resonant interaction, wave generation and cyclical amplitude coupling, were shown. Certainly, the assumption of uniform current is an idealization and capillary and viscous effects will assume importance for large wavenumbers. Nonetheless, results are expected to be indicative of a fundamental behavior of wave-current systems under resonance. Analogous effects may be expected for shearing current which also exhibits multivalued and anisotropic dispersion relations.

The linear wave-current dispersion relation was reviewed in §2. It was shown to be multi-valued and anisotropic. The *existence* of the new resonances was demonstrated using a geometrical approach in §3. Resonance conditions for a laboratory observer are derived in §4. Resonance conditions differ between two wavenumber types (type I and II modes). Generally speaking, slower currents resonate relatively higher frequencies (shorter waves) and higher currents resonate lower frequencies (longer waves) (see Table 3). When the ratio between initial harmonics is known *a priori*, resonance conditions reduce to universal constants of the non-dimensional parameter  $w = \omega U g^{-1}$  (see Table 2). This parameter has been discussed for resonance between waves and an external forcing [cf. Dagan and Miloh, 1982, Tyvand and Torheim, 2012]. The new resonances suggest the parameter is also an indicator of an intrinsic energy sharing mechanism within wave-current fields.

In order to demonstrate physical invariance between inertial observers, resonance conditions are derived for an observer moving with the velocity of the current in §5. The relevant dispersion relations are not

the intrinsic frequencies for all three waves. The dispersion relation for the wave propagating against current still “feels” an ambient motion in the new frame of reference due to the preferential direction of the media. Numerical values for the resonance conditions differ between the laboratory description and observer moving with current. However, it is in the latter that analytical solutions take their simplest form. Thus, the description given by the observer moving with current is preferable for analysis.

In §6, a three-wave interaction model is adapted for triad resonances on current. It is used to demonstrate wave generation and energy exchange between amplitudes. The resonant behavior is dependent on  $\mu$  (ratio of initial harmonics),  $\alpha$  (ratio of initial wave amplitudes), and the permutation  $n$  (wavenumber type). These determine the model parameter  $m_n$  (see fig. 6) which represents the effectiveness of energy transfer to the resonant wave. Current changes are known to modify gravity wave amplitudes [Longuet-Higgins and Stewart, 1960]. It follows, current magnitude will effect resonant behavior *vis a vis* changes in the parameters  $\alpha$  and  $m$ .

Regimes are seen wherein  $\mu$ ,  $\alpha$  and  $m_n$  differ between “small” type I and “large” type II wavenumber scales (see fig. 6). These parameters determine the dominant direction, speed and strength of energy exchange. Since values may be different on two coexisting wavenumber scales, different resonance behaviors may dominate nonlinear energy transfer on different scales simultaneously (compare figs. 7 and 8). This suggests even uniform current is a fundamental source of spatial inhomogeneity.

The results are of both quantitative and qualitative importance. Quantitatively, their quadratic non-linearity will dominate other well known higher-order effects (i.e. quartet interactions). Qualitatively, uniform current was shown to produce significant inhomogeneity. Moreover, the resonances represent a fundamental energy transfer mechanism since they preclude complex 3D effects, topography changes and flow inhomogeneities. Even without considering current inhomogeneities, the results of this paper are the basis for consideration of an even richer dynamics which may be expected for non-collinear wave propagation and capillary effects.

Funding: This research was supported by Israel’s Ministry of Science and Technology [grant No. 3-12473]

## References

- M.R. Alam, Y. Liu, and Dick K.P. Yue. Oblique sub-and super-harmonic bragg resonance of surface waves by bottom ripples. *J. Fluid Mech.*, 643:437–447, 2010.
- F.K. Ball. Energy transfer between external and internal gravity waves. *J. Fluid Mech.*, 19(03):465–478, 1964.
- D.J. Benney. Non-linear gravity wave interactions. *J. Fluid Mech.*, 14(04):577–584, 1962.
- F.P. Bretherton and C.J.R. Garrett. Wavetrains in inhomogeneous moving media. *Proc. R. Soc. Lond. A*, 302(1471):529–554, 1968.
- D. Censor. Dispersion equations in moving media. *P. IEEE*, 68:528–529, 1980.
- D. Censor. Electrodynamics, topsy-turvy special relativity, and generalized minkowski constitutive relations for linear and nonlinear systems. *Progress In Electromagnetics Research*, 18:261–284, 1998.
- G. Dagan and T. Miloh. Free-surface flow past oscillating singularities at resonant frequency. *J. Fluid Mech.*, 120:139–154, 1982.

- T.D. Drivas and S. Wunsch. Triad resonance between gravity and vorticity waves in vertical shear. *Ocean Model.*, 2015.
- J.L. Hammack and D.M. Henderson. Resonant interactions among surface water waves. *Annu. Rev. Fluid Mech.*, 25(1):55–97, 1993.
- K. Hasselmann. On the non-linear energy transfer in a gravity-wave spectrum Part 1. General theory. *J. Fluid Mech.*, 12(04):481–500, 1962.
- U. Kadri and T.R. Akylas. On resonant triad interactions of acoustic-gravity waves. *J. Fluid Mech.*, 788, 2016.
- U. Kadri and M. Stiassnie. Generation of an acoustic-gravity wave by two gravity waves, and their subsequent mutual interaction. *J. Fluid Mech.*, 735, 2013.
- S.A. Kitaigorodskii, V.P. Krasitskii, and M.M. Zaslavskii. On phillips’ theory of equilibrium range in the spectra of wind-generated gravity waves. *J. Phys. Oceanogr.*, 5(3):410–420, 1975.
- D.M. Kouskoulas and Y. Toledo. Effects of dual wavenumber dispersion solutions on a nonlinear monochromatic wave-current field. *Coastal Eng.*, 130:26–33, 2017.
- M.S. Longuet-Higgins. Resonant interactions between two trains of gravity waves. *J. Fluid Mech.*, 12(3):321–332, 1962.
- M.S. Longuet-Higgins and R.W. Stewart. Changes in the form of short gravity waves on long waves and tidal currents. *J. Fluid Mech.*, 8(4):565–583, 1960.
- R. Magne, V. Rey, and F. Ardhuin. Measurement of wave scattering by topography in the presence of currents. *Phys. Fluids*, 17(12):126601, 2005.
- M. McCall and D. Censor. Relativity and mathematical tools: Waves in moving media. *Am. J. Phys.*, 75(12):1134–1140, 2007.
- L.F. McGoldrick. Resonant interactions among capillary-gravity waves. *J. Fluid Mech.*, 21(02):305–331, 1965.
- J.N. Newman. Third-order interactions in kelvin ship-wave systems. *J. Ship Res.*, 15(1), 1970.
- J.N. Newman and P. Schlavounos. The unified theory of ship motions. Technical report, Massachusetts Inst. of Tech. Cambridge dept. of Ocean engineering, 1980.
- D.H. Peregrine. Interaction of water waves and currents. *Adv. appl. Mech.*, 16:9–117, 1976.
- D.H. Peregrine and I.G. Jonsson. Interaction of waves and currents. Technical report, Bristol Univ. (England), 1983.
- O.M. Phillips. On the generation of waves by turbulent wind. *J. Fluid Mech.*, 2(5):417–445, 1957.
- O.M. Phillips. On the dynamics of unsteady gravity waves of finite amplitude part 1. the elementary interactions. *J. Fluid Mech.*, 9(2):193–217, 1960.
- V. Rey, R. Capobianco, and C. Dulou. Wave scattering by a submerged plate in presence of a steady uniform current. *Coast. Eng. J.*, 47(1):27–34, 2002.



- P.D. Schlavounos. *On the diffraction of free surface waves by a slender ship*. PhD thesis, Massachusetts Institute of Technology, 1981a.
- P.D. Schlavounos. The interaction of an incident wave field with a floating slender body at zero speed. Technical report, Massachusetts Institute of Technology, 1981b.
- V.I. Shrira and A.V. Slunyaev. Nonlinear dynamics of trapped waves on jet currents and rogue waves. *Phys. Rev. E*, 89(4):041002, 2014.
- W.F. Simmons. A variational method for weak resonant wave interactions. In *P. Roy. Soc. A Mat.*, volume 309, pages 551–577. The Royal Society, 1969.
- P.A. Tyvand and T. Torheim. Surface waves from bottom vibrations in uniform open-channel flow. *Eur. J. Mech. B-fluid.*, 36:39–47, 2012.
- G.B. Whitham. Mass, momentum and energy flux in water waves. *J. Fluid Mech.*, 12(01):135–147, 1962.

## A Symmetry considerations

Intuitions based on the symmetries of the intrinsic frequency dispersion relation will not hold for water waves propagating on current. The symmetry of the intrinsic frequency dispersion relation,  $\sigma = \sqrt{g|k|}$ , yields

$$\sigma(k) = \sigma(-k) \quad (105)$$

and

$$k(\sigma) = k(-\sigma), \quad (106)$$

All sign changes yield trivial (non-unique) wavenumber solutions; waves in opposite directions are defined by negative wavenumbers with the same magnitude. In practice, these symmetries have lead to simplified sign conventions in defining resonance interaction closures [i.e. Hammack and Henderson, 1993]. However, the symmetries (105) and (106) are not generally true for current. An exhaustive list of the symmetry conditions for wave-current dispersion are not provided here. However, examples are given which demonstrate that (105) and (106) no longer hold.

For waves following current,  $\omega = kU \pm \sqrt{g|k|}$ . Note,  $\omega$  may be understood to be a functional of  $\pm\sigma$  because  $\pm\sqrt{g|k|} = \pm\sigma$ . It follows immediately

$$\omega(k, \sigma(k)) \neq \omega(-k, \sigma(k)). \quad (107)$$

Thus, (105) does not hold for absolute frequencies.

In order to discuss symmetry of the wavenumber solution. Consider a type I mode solution following current, the solution is

$$k_{m1} = \frac{g - 2U\omega - \sqrt{g^2 - 4gU\omega}}{2U^2}. \quad (108)$$

One can see immediately

$$k_{m1}(\omega, U) \neq k_{m1}(-\omega, U). \quad (109)$$

Thus, (106) may be violated due to the preferential direction of the media. Note also, the trivial relationship between wavenumbers for intrinsic frequencies,  $k(\sigma) = k(\sigma)$  is also no longer true for absolute frequencies

$$k_{m1}(\omega_m, U) \neq k_{m1}(\omega_m, -U). \quad (110)$$

As a result of the complex symmetries for waves on current there are non-trivial (unique) solutions for waves propagating in both directions with respect to current. And, the transformation between positive and negative wavenumber conventions is no longer as trivial as it is for the “still” water problem.

## B Positive and negative wavenumber conventions

Assuming only positive  $\omega$ -frequencies, the relative signs of wavenumbers propagating in both directions with respect to current are determined by two possible sign conventions. The first, used in this paper, considers only positive wavenumbers; wave modes propagating in opposite directions with respect to current will both be positive in sign, but are distinguishable as they are functions of opposite signs of  $U$ . In the second convention, the sign of  $U$  is fixed and oppositely directed waves are given by opposite signs of wavenumbers. Mixing signs of  $k$  and  $U$  in any other manner will yield trivial (non-unique) solutions.

### B.1 Positive wavenumbers convention

The positive wavenumber convention is employed in this paper. Signs are chosen such that all wavenumbers are positive; the unique modes for waves propagating in opposite directions are distinguished by opposite signs of  $U$  in their argument. The four wavenumbers for this convention, given in (15), are in explicit form

$$k_{m1} = \frac{g + 2U\omega_m - \sqrt{g(g + 4U\omega_m)}}{2U^2}, \quad (111)$$

$$k_{m2} = \frac{g + 2U\omega_m + \sqrt{g(g + 4U\omega_m)}}{2U^2}, \quad (112)$$

$$k_{m1}^- = \frac{g - 2U\omega_m - \sqrt{g(g - 4U\omega_m)}}{2U^2}, \quad (113)$$

$$k_{m2}^- = \frac{g - 2U\omega_m + \sqrt{g(g - 4U\omega_m)}}{2U^2}. \quad (114)$$

The (-)super-script denotes the wave propagating against current ( $-U$  has been imposed its definition). As written above, all four solutions are functions of positive terms only;  $U, \omega, g > 0$ , and when all solutions are purely real they will also all be positive by definition.

## B.2 Negative and positive wavenumber convention

A convention which permits for negative wavenumbers is also possible. In this convention, waves propagating in different directions with respect to current will have oppositely signed wavenumbers, but are functions of the same sign of  $U$ . The wave-current dispersion relation may be written for this convention as

$$D(\omega, k, U) = \omega^2 - 2k|U|\omega + k^2|U|^2 - g|k| = 0. \quad (115)$$

The positive and negative wavenumbers follow immediately from (115). Solving (115) yields,

$$k_{m1} = \frac{g + 2U\omega - \sqrt{g^2 + 4gU\omega}}{2U^2}, \quad (116)$$

$$k_{m2} = \frac{g + 2U\omega + \sqrt{g^2 + 4gU\omega}}{2U^2}, \quad (117)$$

$$k_{m1}^- = \frac{-g + 2U\omega + \sqrt{g^2 - 4gU\omega}}{2U^2}, \quad (118)$$

$$k_{m2}^- = \frac{-g + 2U\omega - \sqrt{g^2 - 4gU\omega}}{2U^2}. \quad (119)$$

The absolute value of  $U$  is dropped but implied. By definition all wavenumbers are written in terms of positive quantities;  $U, \omega, g > 0$ . And when all solutions are purely two wavenumbers will be positive and two negative *by definition*. The (-)superscript denotes the negative solutions (i.e. waves propagating against current).

Using these nontrivial positive and negative wavenumbers, resonance conditions may be recovered. However, with this choice of sign convention, recovering the triad requires a change in convention in the wave phase definition. Consider type I modes as an example, the triad resonance can be closed for the following phasing between nonlinear and linear terms

$$e^{i(k_m(\omega_m, |U|)x - \omega_m t)} e^{-i(k_p^-(\omega_p, |U|)x + \omega_p t)} \propto e^{i(k_{r1}(\omega_r, |U|)x - \omega_r t)}. \quad (120)$$

The resonance closure is

$$\omega_m + \omega_p = \omega_r, \quad (121)$$

$$k_{m1} + (-k_{p1}^-) = k_{r1}. \quad (122)$$

$k_{p1}^-$  is negative by definition. In order to avoid ambiguity, one may take the absolute value of  $k_{p1}^-$  and reimpose the negatives in (122). It follows,

$$\omega_m + \omega_p = \omega_r, \quad (123)$$

$$k_{m1} + (-(-|k_{p1}^-|)) = k_{r1}. \quad (124)$$

The double negatives yield,

$$\omega_m + \omega_p = \omega_{r1}, \quad (125)$$

$$k_{m1} + |k_{p1}^-| = k_{r1}. \quad (126)$$

Substitute definitions (116) and (118) into (125) and (126) for a self-interaction,  $\omega_m = \omega_p = \omega$  and  $\omega_r = 2\omega_m$ . Resonance is closed when

$$w = \frac{\omega U}{g} = .178. \quad (127)$$

Repeating for type II modes yields the condition  $w = .235$ . These are consistent with the results of §4.

### B.3 Equivalence of conventions

Denote the wavenumber functions for the second convention, (116)-(119), by \*superscripts. Comparing with (111)-(114) recovers the symmetry rules

$$k_{m1} = k_{m1}^*, \quad (128)$$

$$k_{m2} = k_{m2}^*, \quad (129)$$

$$-k_{m1}^- = k_{m1}^{-*}, \quad (130)$$

$$-k_{m2}^- = k_{m2}^{-*}. \quad (131)$$

The two conventions differ only by a trivial sign change for the waves propagating against current.

## C Doppler shift of the resonance closure for waves propagating in opposite directions on current

For a single plane wave, given by a laboratory description, application of a Doppler shift yields an intrinsic frequency and *vice versa*. It does not follow that uniform application of a Doppler shift to a triad resonance closure will always reproduce the resonance closure in terms of intrinsic frequencies. In particular, this assumption is not true for a triad resonance between wave modes propagating in opposite directions with respect to a current (see laboratory description in §4). This is demonstrated in the following derivation..

The frequency closures for a triad resonance between absolute and intrinsic frequencies are

$$\omega_m + \omega_p^- = \omega_r, \quad (132)$$

$$\sigma_m + \sigma_p = \sigma_r, \quad (133)$$

respectively. A positive wavenumber convention is employed (see Appendix B for a discussion of sign conventions), the  $(-)$ super-script denotes the wave mode propagating against current.

As a first step, one can inspect the three independent plane waves in the same laboratory reference frame. Introducing current into the velocity potential yields  $(\omega^\mp) \pm kU = \sigma$ . Accordingly, the components of (132) and (133) are related by

$$\begin{bmatrix} \omega_m \\ \omega_p \\ \omega_r \end{bmatrix} = \begin{bmatrix} \sigma_m \\ \sigma_p \\ \sigma_r \end{bmatrix} + \begin{bmatrix} 1 & 0 & 0 \\ 0 & -1 & 0 \\ 0 & 0 & 1 \end{bmatrix} U \begin{bmatrix} k_m \\ k_p^- \\ k_r \end{bmatrix}. \quad (134)$$

Equation (134) is the laboratory description for the three waves on the same current. Since a positive wavenumber convention is employed,  $-U$  is required to capture the wave propagating against current (for a negative wavenumber convention, all values of  $U$  are positive but the wavenumber is negative and similar results follow).

The second step is to apply the same Doppler shift moving with the velocity  $U$  to each frequency component in (134). This yields

$$\begin{aligned} \begin{bmatrix} \sigma_m \\ \sigma_p \\ \sigma_r \end{bmatrix} + \left( \begin{bmatrix} 1 & 0 & 0 \\ 0 & -1 & 0 \\ 0 & 0 & 1 \end{bmatrix} - \begin{bmatrix} 1 & 0 & 0 \\ 0 & 1 & 0 \\ 0 & 0 & 1 \end{bmatrix} \right) U \begin{bmatrix} k_m \\ k_p^- \\ k_r \end{bmatrix} \\ = \begin{bmatrix} \sigma_m \\ \sigma_p \\ \sigma_r \end{bmatrix} + \begin{bmatrix} 0 & 0 & 0 \\ 0 & -2 & 0 \\ 0 & 0 & 0 \end{bmatrix} U \begin{bmatrix} k_m \\ k_p^- \\ k_r \end{bmatrix} \neq \begin{bmatrix} \sigma_m \\ \sigma_p \\ \sigma_r \end{bmatrix}. \end{aligned} \quad (135)$$

The intrinsic frequencies of all three waves are *not* recovered. In (132), the doppler-shifted frequency of the wave propagating against current is  $\sigma_p - 2Uk_p$ . This wave feels a drag  $\propto 2U$  due to the preferential direction of the media. This highlights a difficulty in treating a multi-wave systems on current, since the doppler shift cannot be used to cancel the current effect for components propagating in opposite directions with respect to current.

In order to avoid conflating this description with the intrinsic frequency description, one may introduce a  $v$ -frequency definition,

$$\begin{bmatrix} v_m \\ v_p \\ v_r \end{bmatrix} = \begin{bmatrix} \sigma_m \\ \sigma_p \\ \sigma_r \end{bmatrix} + \begin{bmatrix} 0 & 0 & 0 \\ 0 & -2 & 0 \\ 0 & 0 & 0 \end{bmatrix} U \begin{bmatrix} k_m \\ k_p^- \\ k_r \end{bmatrix}. \quad (136)$$

$v$ -frequencies are defined for an observer who moves at the current velocity, according to the Doppler shift applied in (135), and accounts for the preferential direction of the media. The  $v$ -description is not exactly equivalent to three intrinsic frequencies. The dependency of (136) on intrinsic frequencies is eliminated by introducing *local* definitions for intrinsic frequencies:  $\sigma_i = \sqrt{gk_i}$ . This yields

$$\begin{bmatrix} v_m \\ v_p \\ v_r \end{bmatrix} = \begin{bmatrix} \sqrt{gk_m} \\ \sqrt{gk_p^-} \\ \sqrt{gk_r} \end{bmatrix} + \begin{bmatrix} 0 & 0 & 0 \\ 0 & -2 & 0 \\ 0 & 0 & 0 \end{bmatrix} U \begin{bmatrix} k_m \\ k_p^- \\ k_r \end{bmatrix}. \quad (137)$$

Rearranging (137) yields the following system of equations

$$v_m^2 - gk_m = 0, \quad (138)$$

$$(v_p^- + 2k_p^- U)^2 - gk_p^- = 0, \quad (139)$$

$$v_r^2 - gk_r = 0. \quad (140)$$

These are the dispersion relations which follow from (56) in §5. In §5, triad resonances were found between  $v$ -frequencies.

## D Nonlinear terms and secular growth

The nonlinear operator is

$$\begin{aligned} \mathcal{P}^2(\tilde{\phi}, \tilde{\phi}) = & \frac{1}{g^2} \left( - \left( \frac{\partial^2 \phi}{\partial t^2} + 2U \frac{\partial^2 \phi}{\partial x \partial t} + U^2 \frac{\partial^2 \phi}{\partial x^2} - g \frac{\partial \phi}{\partial z} \right) \left( U \frac{\partial^2 \phi}{\partial x \partial z} + \frac{\partial^2 \phi}{\partial z \partial t} \right) \right. \\ & - \frac{\partial \phi}{\partial t} \left( U^2 \frac{\partial^3 \phi}{\partial x^2 \partial z} + 2U \frac{\partial^3 \phi}{\partial x \partial z \partial t} + \frac{\partial^3 \phi}{\partial t^2 \partial z} + g \frac{\partial^2 \phi}{\partial z^2} \right) + \frac{\partial \phi}{\partial x} \left( 2g \frac{\partial^2 \phi}{\partial x \partial t} \right. \\ & \left. \left. - U \left( -2g \frac{\partial^2 \phi}{\partial x^2} + g \frac{\partial^2 \phi}{\partial z^2} + U^2 \frac{\partial^3 \phi}{\partial x^2 \partial z} + 2U \frac{\partial^3 \phi}{\partial x \partial z \partial t} + \frac{\partial^3 \phi}{\partial t^2 \partial z} \right) \right) \right). \end{aligned} \quad (141)$$

Secular growth in quadratic nonlinear interactions due to resonant phase matching is seen using the approach of Phillips [1957], Benney [1962]. One must define a kinematic equation governing the “slow” generation of a resonant wave  $b_{rs}$  through the nonlinear interaction of  $b_{mn}$  and  $b_{pq}^-$ . Equations (10), (141) and (21) yield the nonlinear governing equation of the form given by (9).

Among linear terms, retain only those involving  $b_{rs}$  (the generated wave). Among nonlinear terms, retain only those  $\propto e^{i((k_{mn} + k_{pq}^-)x - (\omega_m + \omega_p)t)}$ . Let  $b_{rs}$  be a function of a “slow” time  $\tau = \varepsilon t$  (i.e.  $b_{rs} = b_{rs}(\tau)$ ). According to Resonant Interaction Theory, non-resonant terms may be assumed to remain of negligible order. Upon rearranging, growth of the resonant wave in slow time may be written in the form

$$\frac{db_{rs}}{d\tau} = W_{mn,pq,rs} b_{mn} b_{pq}^- e^{i((k_{mn} + k_{pq}^- - k_{rs})x - (\omega_m + \omega_p - \omega_{rs})t)}. \quad (142)$$

Wherein,

$$\begin{aligned} W_{mn,pq,rs} = & \frac{1}{(gk_{rs} - (\omega_r - k_{rs}U)^2)} \left( (k_{mn} + k_{pq}) (k_{mn}U + \omega_{mn}) (k_{pq}U + \omega_{pq})^2 \right. \\ & \left. - gk_{pq} (k_{mn}^2 U - k_{pq}\omega_{mn} - k_{mn} (k_{pq}U + \omega_{mn} + 2\omega_{pq})) \right). \end{aligned} \quad (143)$$

Equation (143) is the quadratic nonlinear interaction coefficient produced by the velocity potential (21). As expected, the dispersion relation appears in the denominator and a standard perturbation will fail at exact resonance. It is reassuring the bound wave solution given in Kadri and Stiassnie [2013] may be recovered by noting  $b \propto ig(2\omega)^{-1}a$  and letting  $U = 0$ .

Equation (142) and (143) suggests resonance causes secular growth of nonlinear terms over slow time. Secular growth is nonphysical. However, equation (142) may be understood to represent an initial growth rate of  $b_{rs}$  from zero [Phillips, 1957, 1960]. In order to advance the model to a greater level of realism, all three amplitudes may be permitted to be functions of the slow time. Amplitude coupling is then seen to arrest the secular growth [cf. Benney, 1962, McGoldrick, 1965]. Nonetheless, if the interaction time is sufficiently long, nonlinear terms may still grow to first-order magnitude (see §6).

## E Exact solution for a laboratory viewer

For a laboratory viewer, the frequency condition for resonance is (see §4)

$$4\mu w_{mn} + \sqrt{1 - 4\mu w_{mn}} + \sqrt{4w_{mn} + 1} = \sqrt{4(\mu + 1)w_{mn} + 1} + 1. \quad (144)$$

An exact solution is given by

$$w_{mn} = -\frac{\sqrt{\beta}}{2} + \frac{1}{2\mu^2} + \frac{1}{2\mu} - (-1)^n \frac{\sqrt{\alpha}}{2}, \quad n = 1, 2. \quad (145)$$

Wherein,

$$\begin{aligned} \alpha = & \frac{1}{4\sqrt{\beta}} \left( \frac{18}{\mu^3} + \frac{54}{\mu^4} + \frac{56}{\mu^5} + \frac{16}{\mu^6} \right) - \frac{4\sqrt[3]{2}}{3\gamma} \left( \frac{4}{\mu^2} + \frac{16}{\mu} + 22 + 12\mu + 3\mu^2 \right) \\ & + \frac{1}{\mu^2} + \frac{5}{3\mu^3} + \frac{4}{3\mu^4} - \frac{\gamma}{48\sqrt[3]{2}\mu^6}, \end{aligned} \quad (146)$$

$$\beta = \frac{4\sqrt[3]{2}}{3\gamma} \left( \frac{4}{\mu^2} + \frac{16}{\mu} + 22 + 12\mu + 3\mu^2 \right) - \frac{1}{3\mu^3} + \frac{1}{3\mu^4} + \frac{\gamma}{48\sqrt[3]{2}\mu^6}, \quad (147)$$

$$\begin{aligned} \gamma = & (8192\mu^6 + 49152\mu^7 + 116736\mu^8 + 139264\mu^9 + 89856\mu^{10} \\ & + 32256\mu^{11} + 6912\mu^{12} + \delta)^{\frac{1}{3}}, \end{aligned} \quad (148)$$

$$\begin{aligned} \delta = & (28311552\mu^{18} + 169869312\mu^{19} + 401670144\mu^{20} + 474218496\mu^{21} \\ & + 300810240\mu^{22} + 106168320\mu^{23} + 19464192\mu^{24})^{\frac{1}{2}}. \end{aligned} \quad (149)$$

For a self-interaction ( $\mu = 1$ ), this reduces to

$$w_{mn} = \frac{1}{12} \left( 12 + (-1)^n 3^{2/3} \sqrt{96\sqrt{\frac{1}{\aleph}} - \aleph - 3^{2/3}\sqrt{\aleph}} \right). \quad (150)$$

Wherein,

$$\aleph = 38\sqrt[3]{\frac{3}{144 + \sqrt{159}}} + 2\sqrt[3]{144 + \sqrt{159}}.$$